JOURNAL OF THERMOPHYSICS AND HEAT TRANSFER
Vol. 18, No. 2, April–June 2004

Effect of Rotation on Heat Transfer in Rectangular Channels with Pin Fins

Lesley M. Wright,* Eungsuk Lee,* and Je-Chin Han†
Texas A&M University, College Station, Texas 77843-3123

The effect of rotation on smooth narrow rectangular channels and narrow rectangular channels with pin fins is investigated in this study. Pin fins are commonly used in the narrow sections within the trailing edge of the turbine blade; the pin fins act as turbulators to enhance internal cooling while providing structural support in this narrow section of the blade. The rectangular channel is oriented at 150 deg with respect to the plane of rotation, and flow through the channel is radially outward. The focus of the study involves narrow channels with aspect ratios of 4:1 and 8:1. The enhancement due to both conducting (copper) pin fins and nonconducting (Plexiglas®) pins is investigated. Because of the varying aspect ratio of the channel, the height-to-diameter ratio (h_p/D_p) of the pins varies from two, for an aspect ratio of 4:1, to unity, for an aspect ratio of 8:1. A staggered array of pins with uniform streamwise and spanwise spacing ($x_p/D_p = s_p/D_p = 2.0$) is studied. With this array, 42 pin fins are used, giving a projected surface density of 3.5 pins/in.^{2} (0.543 pins/cm^2), for the leading or trailing surfaces. The range of flow parameters include Reynolds number ($Re_{Dh} = 5 \times 10^3$–2×10^4), rotation number ($Ro = 0.0$–0.302), and inlet coolant-to-wall density ratio ($\Delta\rho/\rho = 0.12$). Heat transfer in a stationary pin fin channel can be enhanced up to 3.8 times that of a smooth channel. Rotation enhances the heat transferred from the pin fin channels to 1.5 times that of the stationary pin fin channels. Overall, rotation enhances the heat transfer from all surfaces in both the smooth and pin fin channels. Finally, as the rotation number increases, spanwise variation increases in all channels.

Nomenclature

A	=	convecting surface area, m^2
$A_{c,b}$	=	cross-sectional area of pin, m^2
A_{con}	=	surface area in conducting pin fin channel, m^2
$A_{\text{cu,pl}}$	=	surface area of copper plate, m^2
A_{nc}	=	surface area in nonconducting pin fin channel, m^2
A_p	=	surface area of pin fin, m^2
D_h	=	hydraulic diameter, m
D_p	=	pin diameter, m
h	=	heat transfer coefficient, W/m^{2}K
h_p	=	pin height, m
k	=	thermal conductivity of coolant, W/mK
L	=	length of duct, m
Nu	=	regionally averaged Nusselt number, hD_h/k
Nu_{D_p}	=	Nusselt number for channel flow through a staggered array of pin fins, hD_p/k
Nu_0	=	Nusselt number for flow in fully developed turbulent nonrotating smooth tube
Pr	=	Prandtl number
Q	=	rate of heat transfer, W
Q_{net}	=	net rate of heat transfer, W
R	=	mean rotating arm radius, m
Re_{D_h}	=	Reynolds number based on hydraulic diameter, $\rho V D_h/\mu$
Re_{D_p}	=	Reynolds number based on pin diameter and maximum velocity, $\rho V_{\max} D_p/\mu$
Ro	=	rotation number, $\Omega D_h/V$
s_p	=	spanwise pin spacing, m
$T_{b,x}$	=	local coolant bulk temperature, K
T_w	=	wall temperature, K
V	=	bulk velocity in streamwise direction, m/s
$V_{\max}$	=	maximum bulk velocity in streamwise direction, m/s
x	=	streamwise location, m
x_p	=	streamwise pin spacing, m
β	=	angle of channel orientation
ρ	=	density of coolant, kg/m^3
$\Delta\rho/\rho$	=	inlet coolant-to-wall density ratio, $(\rho_{b,i} - \rho_w)/\rho_{b,i}$, $(T_w - T_{b,i})/T_w$
Ω	=	rotational speed, rad/s

Received 20 August 2003; revision received 17 October 2003; accepted for publication 18 October 2003.

*Graduate Research Assistant, Turbine Heat Transfer Laboratory, Department of Mechanical Engineering.

†M.C. Easterling Chair Professor, Turbine Heat Transfer Laboratory, Department of Mechanical Engineering. Associate Fellow AIAA.

Introduction

THERE is an increasing demand for energy throughout the world, and to meet this increasing demand, the turbomachinery industry developed more efficient ways of generating power. Gas turbines play a significant role in society; they are vital for power generation, aircraft propulsion, and numerous other industrial applications. One method used to increase the efficiency of these turbines is to increase the gas inlet temperature; however, when the gas temperature is raised, the structural integrity of the turbine blades is compromised. For the blades to withstand the extremely high inlet temperatures, they must be manufactured from superior materials, have an excellent cooling design, or both. One method for cooling the blades is internal cooling. With internal blade cooling, a small amount of air is extracted from the compressor, and the air is injected into the blades. Through forced convection, the coolant air removes heat from the wall of the blade.

The narrow trailing edge of the turbine blade poses many challenges from both a cooling and manufacturing view. The trailing edge is very narrow, and so the typical cooling techniques of jet impingement and ribbed channels cannot be employed due to manufacturing constraints. Pin fins provide solutions to these problems. The pin fins enhance heat transfer by turbulating the coolant air passing through the channel while increasing the structural integrity within this narrow section of the blade. Because of manufacturing constraints and the geometry of the channel, pin fins typically have a height-to-diameter ratio close to one.

The flowfield through a rotating channel exhibits different characteristics than the flowfield through a stationary channel. This is due to the forces generated by rotation. These Coriolis and rotational

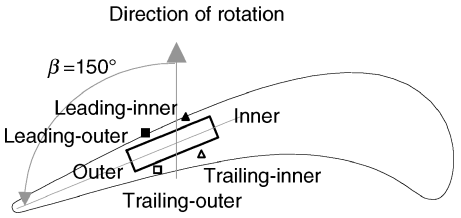

Fig. 1 Orientation of narrow rectangular channel in a gas turbine blade.

buoyancy forces shift the velocity profile of the coolant toward the trailing surface (pressure side) of the blade. Therefore, the coolant is forced away from the leading surface (suction side) of the channel to the trailing surface. Typically, under rotation, the trailing surface experiences heat transfer enhancement, whereas the leading surface experiences a reduction in heat transfer.

The duct orientation and aspect ratio also have an effect on the coolant flow through the channel. As one moves from the midchord of the blade toward the trailing edge, the blade becomes thinner; therefore, cooling channels must become narrower. (The aspect ratio increases.) Movement toward the trailing edge of the blade also alters the orientation angle β of the cooling channel. Movement from the midchord toward the trailing edge, increases the orientation angle (measured from the direction of rotation to the midpoint of the channel). For narrow ducts with large orientation angles, the coolant is forced away from leading and inner surfaces toward the trailing and outer surfaces of the channel during rotation. Figure 1 shows the orientation of an 8:1 aspect ratio channel within the trailing edge of a turbine blade.

As the power industry has evolved over the past several decades, the research efforts focusing on rotor blade efficiency and reliability have also evolved. Early studies investigated stationary channels with limited variation in the channel geometry. The geometry of the channels became more complex to maximize the heat transfer from the blades. To simulate actual turbine conditions more closely, the effect of rotation in cooling channels became the focus of many studies.

Wagner et al.[1] studied the effect of rotation on a smooth square channel with radial outward flow. They found that as the rotation number increased, the heat transfer from the leading surface decreased significantly; the heat transfer decreased by as much as 40% when compared to stationary smooth channels. However, the trailing surface underwent heat transfer enhancement; the heat transfer was enhanced up to 3.5 times that of a smooth stationary duct.

Many other studies have shown the same trends for the leading and trailing surfaces of square channels. However, the studies that involved square channels are not applicable to the narrow rectangular channels located in the trailing-edge portion of the blade. The heat transfer trends in the narrow channels will vary from the trends in the square ducts. These narrow channels, with various orientation angles, will have secondary flow behavior, unlike that of the square channel, due to the Coriolis and rotational buoyancy forces. More recent studies have focused on these narrow channels with various orientation angles.

Dutta et al.[2] studied the effect of rotation in a triangular two-pass duct with smooth walls. They found that as the rotation number increased, the trailing surface of the duct experienced heat transfer enhancement, whereas the heat transfer from the leading surface decreased (as compared to stationary channels).

A narrow rectangular rotating channel ($AR = 10{:}1$) oriented at 60 deg to the R–Z plane was studied by Willet and Bergles.[3] Their study, which primarily focused on the buoyancy effect inside the channel, found the normalized Nusselt number ratio in this duct is a strong function of rotation number and buoyancy number. They also observed significant spanwise variation in the Nusselt number ratio under rotating conditions.

Griffith et al.[4] recently studied narrow rectangular channels ($AR = 4{:}1$) oriented at 135 deg with respect to the plane of rotation. They found the duct orientation has a significant effect on the leading, inner, and outer surfaces of the smooth rotating channel; however, the effect of rotation on the trailing surface is minimal. This study also showed that the Nusselt number ratio can vary as much as 25% in the spanwise direction.

The use of pin fins to enhance heat transfer in cooling channels has been the focus of many studies throughout the years. However, the majority of investigations that involved pin fins have been limited to stationary channels. Metzger et al.[5] studied the developing heat transfer of short pin fins in stationary staggered arrays. They observed that the heat transfer coefficient gradually increases over the first several rows of pins, reaches a maximum around the third row, and gradually decreases through the remaining rows of the array. Metzger and Haley[6] then studied the effects of pin material and pin spacing on heat transfer in staggered arrays. They found that the Nusselt number values for the nonconducting pin fins closely followed the values of the conducting pin fins. They also showed that, as the streamwise spacing (x_p/D_p) increased, the Nusselt number values decreased. Later, Metzger et al.[7] examined the row resolved heat transfer variation in pin-fin arrays. From this study, they developed the following well-known correlation:

$$Nu_{D_p} = 0.135 Re_{D_p}^{0.69} (x_p/D_p)^{-0.34} \tag{1}$$

This equation was developed while the copper pins with a spanwise spacing of $s_p/D_p = 2.0$ were studied and it is applicable to streamwise spacing of $1.5 \leq x_p/D_p \leq 5.0$ and height-to-diameter ratios of $0.5 \leq h_p/D_p \leq 3.0$.

VanFossen[8] also investigated stationary cooling channels with pin fin arrays. This study showed that the heat transfer from an array of short pins is lower than the heat transfer from an array of long pins. From this study, it was also found that the heat transfer coefficients on the pin surface were approximately 35% greater than those on the endwall. Finally, it was determined that the existing correlations for pin fin heat transfer, which contain terms to account for the pin length, do not represent adequately the heat transferred from short pins. In a later study, Brigham and VanFossen[9] concluded that the pin height-to-diameter ratio (h_p/D_p) is the dominant factor affecting the amount of heat transferred from short pin fin arrays (endwalls included). They also found that for height-to-diameter ratios less than two, the Nusselt number is only a function of the Reynolds number. For longer pins ($h_p/D_p > 2$), the Nusselt number is a function of both Reynolds number and the height-to-diameter ratio.

In more recent studies, Chyu and Hsing[10] examined the heat transfer of cubic fin arrays. They concluded that the cubic pin fin yields the highest heat transfer (in both staggered and inline arrays), followed by diamond, and then circular pin fins. However, because of the ease of manufacturing, the circular pin fin is more commonly used in the turbine blade cooling channels. Chyu et al.[11] also studied the heat transfer contribution of pin fins and endwalls in pin fin arrays. This study found that conducting pin fins have a significantly higher heat transfer coefficient (10–20%) than the endwalls. This study also yielded separate correlations for the heat transfer from the pins, the endwall, and the average of the pin and endwall surfaces. These correlations showed a greater dependence on the Reynolds number as compared to a previous correlation developed by Metzger et al.[5]

Uzol and Camci[12] recently investigated the endwall heat transfer and total pressure loss within various arrays of pin fins. This investigation used a liquid crystal technique to measure the endwall heat transfer downstream of two rows of fins. This study compared the heat transfer enhancement of circular pins and two elliptical pin fin arrays. They found that the heat transfer in the wake of the circular pins is 25% higher than that of the elliptical arrays; however, the elliptical geometry is viewed as more desirable configuration due to the reduced pressure drop (when compared to the circular array).

In an experiment conducted by Willett and Bergles,[13] the heat transfer in rotating channels with conducting pin fins was studied ($AR = 10{:}1$). They found that the heat transfer enhancement due to rotation and buoyancy was much less than the enhancement observed from their study of a smooth narrow duct.[3] They showed that pin fins significantly reduce the effect of rotation, but they do not eliminate the effect.

Table 1 Experimental case summary

Channel geometry	Aspect ratio	Hydraulic diameter, in. (cm)	D_p, in. (cm)	h_p, in. (cm)	h_p/D_p	x_p/D_p	s_p/D_p
Smooth	4:1	0.80 (2.03)	——	——	——	——	——
Smooth	8:1	0.44 (1.13)	——	——	——	——	——
Nonconducting pin fins	4:1	0.80 (2.03)	0.25 (0.635)	0.5 (1.27)	2.0	2.0	2.0
Nonconducting pin fins	8:1	0.44 (1.13)	0.25 (0.635)	0.25 (0.635)	1.0	2.0	2.0
Conducting pin fins	4:1	0.80 (2.03)	0.25 (0.635)	0.5 (1.27)	2.0	2.0	2.0

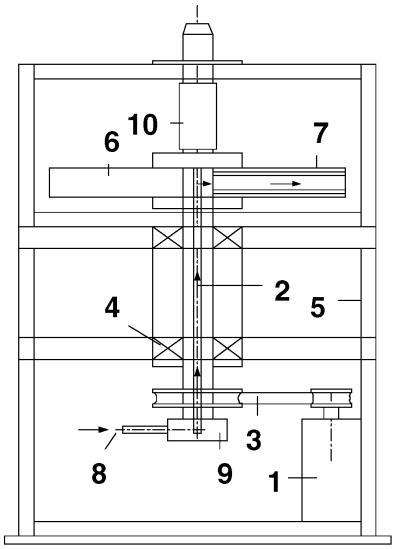

Fig. 2 Rotating test facility: 1) variable speed electric motor, 2) hollow rotating shaft, 3) belt-driven gear system, 4) bearing support system, 5) steel work table, 6) rotating arm, 7) test section, 8) compressor air, 9) rotary seal, and 10) slip ring assembly.

A comprehensive review of internal turbine blade cooling is given by Han et al.[14]

The present study explores the effect of rotation on the regionally averaged heat transfer coefficients in narrow channels with radially outward flow. Both conducting and nonconducting pin fins are investigated in this study. The study addresses the spanwise heat transfer variation on both the leading and trailing surfaces, as well as the streamwise variation due to the staggered array of pin fins. The effect of variation of the channel aspect ratio is also explored in this study.

Experimental Facility

The experimental test rig used for this study was previously used by Griffith et al.[4] and is shown in Fig. 2. A variable frequency motor is used to rotate a hollow shaft by the utilization of a gear-and-belt mesh. The hollow shaft extends from the base of the test rig to the work platform. A hollow rotating arm is attached orthogonal to the rotating shaft; the test section is inserted into this rotating arm. Thermocouple and heater wires are connected to a 100-channel slip ring assembly that is mounted to the rotating shaft. The thermocouple output is monitored with commercially available software. The temperature data are displayed with the virtual instrument format, and the data are written to a data file specified by the user. Power is supplied through the slip ring to the heaters by the use of variable transformers. Cooling air is pumped to the test rig with a steady flow air compressor. The air flows through an American Society of Mechanical Engineers square-edge orifice meter, upward through the hollow rotating shaft, around a 90-deg bend, through two mesh screens, and into the rotating arm and test section. After it flows through the test section, the air is expelled to the atmosphere.

The test section is a one-pass rectangular channel. The ratio of mean rotating arm radius-to-channel hydraulic diameter ($\bar{R}/D_h$) is 33.0 and 59.4 for the 4:1 and 8:1 channels, respectively. Likewise, the heated channel length-to-hydraulic diameter ratio (L/D_h) is 7.5 for the 4:1 channel and 13.5 for the 8:1 channel. The air flows radially outward from the axis of rotation through the test section.

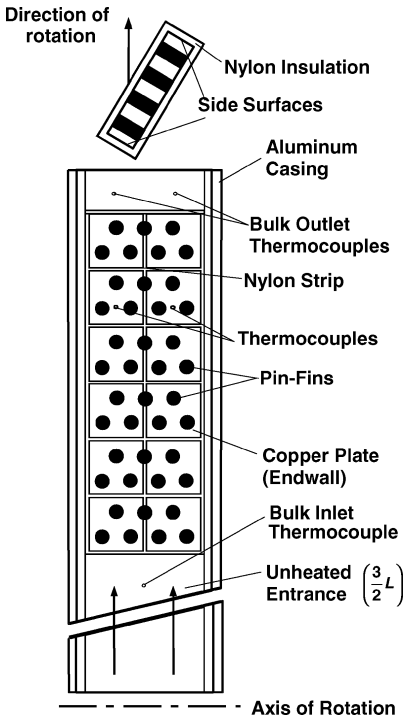

Fig. 3 Schematic of the pin fin test section.

Figure 3 is a schematic of the test section used in the present study. The test section consists of the leading, trailing, inner, and outer surfaces. The inner and outer surfaces each consist of six plates in the streamwise direction. The leading and trailing surfaces each consist of 12 plates. The cross section of the test section contains two plates for the leading surface, two plates for the trailing surface, one plate for the inner surface, and one plate for the outer surface. A total of 36 copper plates make up the entire test section. Each plate is surrounded by a 0.0625-in. (0.159-cm) strip of nylon to prevent conduction between the plates. This provides a grid for analysis of the spanwise variation in the regionally averaged heat transfer coefficients.

Each 0.125-in.- (0.318-cm-) thick copper plate has a 0.0625-in.- (0.159-cm-) deep blind hole drilled in its backside. The temperature of each copper plate is measured using a 36-gauge type T thermocouple. The thermocouple is secured in the blind hole with thermally conductive epoxy. With this setup, the thermocouple junction is located 0.0625 in. (0.159 cm) from the surface of the copper plate.

A nylon substrate serves as the support for the test section; each of the copper plates is mounted into this substrate. Flexible heaters are installed beneath the leading and trailing surfaces, two for each surface. Thermal conducting paste is applied between the heater and copper plates to minimize contact resistance and promote heat transfer from the heater to the plates. The outer and inner walls (or sidewalls) are smooth, and they are unheated.

Table 1 lists the channel geometries used in this study. Both conducting (copper) and nonconducting (Plexiglas®) pins are used in this study. The height-to-diameter ratio of the pins varies from 1 to 2 depending on the channel aspect ratio. As shown in Fig. 3, the pins are arranged in a staggered array with uniform spanwise and streamwise spacing ($s_p/D_p = x_p/D_p = 2.0$). The channel consists of smooth copper plates, and so the pins are attached to the smooth

Table 2 Reynolds numbers and corresponding rotation numbers for 4:1 and 8:1 channels

Reynolds number Re_{D_h}	Rotation number, $AR = 4{:}1$	Rotation number $AR = 8{:}1$
5×10^3	0.302	0.093
1×10^4	0.150	0.046
1.5×10^4	0.100	0.031
2×10^4	0.075	0.023

plates of the leading and trailing surfaces. For the 8:1 channel, the 0.25-in.- (0.635-cm-) long nonconducting pins are attached to the leading surface with tape, and they are attached to the tailing surface with super glue. This minimizes the conduction between the copper plates and the Plexiglas pin fins, and it allows the test section to be easily disassembled after the experiment is completed. For the 4:1 channel with nonconducting pin fins, two Plexiglas pins (each 0.25 in. long) are super glued together. The 0.5-in.- (1.27-cm-) long nonconducting pin is then glued and taped to the test section, as were the 0.25-in. (0.625-cm) Plexiglas pins.

The conducting pins are attached to the test section in a different manner. Each half of the pin fin is glued to the test section with epoxy with a high thermal conductivity. A thin layer of tape is then placed between the pin halves. The tape ensures that the two halves of the pin are in contact and that no gaps exist between the pin halves. Because the base of the pins is glued directly to the smooth surface, the layer of tape allows for the test section to be easily disassembled on completion of the test. The tape also reduces heat conduction between the leading and trailing surfaces.

The test section is oriented at 150 deg from the direction of rotation (Fig. 1). The experiments are conducted at Reynolds numbers (based on the hydraulic diameter) of 5×10^3, 1×10^4, 1.5×10^4, and 2×10^4. Constant heat flux is supplied to the test section by each of the heaters. The maximum wall temperature is maintained at approximately 38°C above the inlet coolant temperature to yield an inlet coolant-to-wall density ratio ($\Delta\rho/\rho$) of approximately 0.12 for all cases. The rotation speed remained constant at 550 rpm, which resulted in a range of rotation number Ro from 0.023 to 0.302. Table 2 presents the Reynolds numbers and the corresponding rotation numbers for the 4:1 and 8:1 cooling channels.

Data Reduction

The purpose of this investigation is to study the regionally averaged heat transfer coefficient at various locations within a narrow rotating duct with pin fins. The heat transfer coefficient is determined by the net heat transferred from the heated plate, the surface area of the plate, the regionally averaged temperature of the plate, and the local bulk mean temperature in the channel. Therefore, the heat transfer coefficient is given as

$$h = \frac{Q_{\text{net}}/A}{(T_w - T_{b,x})} \tag{2}$$

The net heat transfer is calculated by the use of the measured voltage and current supplied to each heater from the variac transformers, multiplied by the area fraction of the heater exposed to the respective plate, minus the external heat losses escaping from the test section. The heat losses are predetermined by the performance of a heat loss calibration for both the rotational and stationary experiments. The heat loss calibration is performed by the insertion of insulation into the channel to eliminate natural convection. During the calibration, the heat transfer (in the form of power from the variac transformers) and wall temperature of each plate is measured; therefore, from the conservation of energy principle, it is possible to know how much heat is being lost to the environment.

The surface area used in this study is dependent on the type of pin fin being studied. In the cases of the nonconducting (Plexiglas) pins, the surface area is taken as the projected surface area of the channel, that is, the smooth channel area, $A_{\text{nc}} = A_{\text{cu,pl}}$. In this case, the actual convecting area is less than the area given for the smooth duct due to the Plexiglas pins. Because the actual convecting area is less than the total copper area used, the calculated net heat transfer flux is less than the actual heat transfer flux from only the exposed copper area. In the present study, the exposed copper convecting area is approximately 17% less than the smooth channel area. When the conducting (copper) pin fins are studied, the surface area is taken as the area of the exposed copper. Therefore, the surface area includes the surface area of the pin fins ($A_{\text{con}} = A_{\text{cu,pl}} + A_p - A_{c,b}$). By the use of these surface area definitions, a better representation of the regional heat transfer coefficient is presented.

Table 3 Comparison of Reynolds numbers based on hydraulic diameter and pin diameter

Reynolds number Re_{D_h}	Reynolds number Re_{D_p}, $AR = 4{:}1$	Reynolds number Re_{D_p}, $AR = 8{:}1$
5×10^3	3.107×10^3	5.622×10^3
1×10^4	6.261×10^3	1.1264×10^4
1.5×10^4	9.426×10^3	1.7038×10^4
2×10^4	1.2539×10^4	2.2604×10^4

The regionally averaged wall temperature T_w is directly measured with the thermocouple installed in the blind hole on the backside of each copper plate. Linear interpolation is used to determine the local bulk temperature. One thermocouple at the inlet and two thermocouples at the outlet of the test section measure the inlet and outlet bulk temperatures, respectively. Therefore, the bulk temperature at any location in the test section can be calculated by the use of linear interpolation. However, the local bulk temperature can also be calculated with the conservation of energy principle. For the present study, both methods compare very well; the difference between the two methods is less than 5%. The energy balance equation is

$$T_{b,x} = T_{\text{in}} + \sum_i \frac{(Q - Q_{\text{loss}})}{mc_p}, \qquad x = 1, 2, \ldots, 6 \tag{3}$$

The Dittus and Boelter/McAdams correlation for heating ($T_w > T_{b,x}$) is used in this study to provide a basis of comparison. The correlation is used to calculate the Nusselt number for fully developed turbulent flow through a smooth stationary circular tube. Therefore, the Nusselt number ratio is given as

$$Nu/Nu_0 = (hD_h/k)\left(1/0.023Re_{D_h}^{0.8}Pr^{0.4}\right) \tag{4}$$

To provide consistent comparisons for future studies, both the Nusselt number obtained from the experiment and the Dittus and Boelter/McAdams correlation are based on the hydraulic diameter of the duct. Table 3 shows the comparison between the Reynolds numbers based on the hydraulic diameter and the pin diameter for both channel aspect ratios ($AR = 4{:}1$ and 8:1). All air properties are taken based on the bulk air temperature with a Prandtl number Pr for air of 0.71.

The experimental uncertainty for the presented results was calculated with the method developed and published by Kline and McClintock.[15] At the Reynolds number of 5×10^3, where the most uncertainty exists in the measured quantities, the overall uncertainty in the Nusselt number ratio is approximately 20% of the presented values. However, at the higher Reynolds numbers, the percent uncertainty of the individual measurements decreases, and the overall uncertainty in the Nusselt number ratio decreases to approximately 12% of the calculated value at the highest Reynolds number of 2×10^4.

Results and Discussion

The legend for the present channel is shown in Fig. 1. The inner surface is the surface located closest to the midchord of the blade, and the outer surface is the surface located closest to the trailing edge of the blade. The leading and trailing surfaces are each subdivided into two surfaces. The leading surface is divided into the leading-inner surface and the leading-outer surface, and the same is done for the trailing surface. With the narrow channels used in the trailing edge of the blade, the heat transfer from the inner and outer surface is much lower than the contribution of the leading and trailing surfaces;

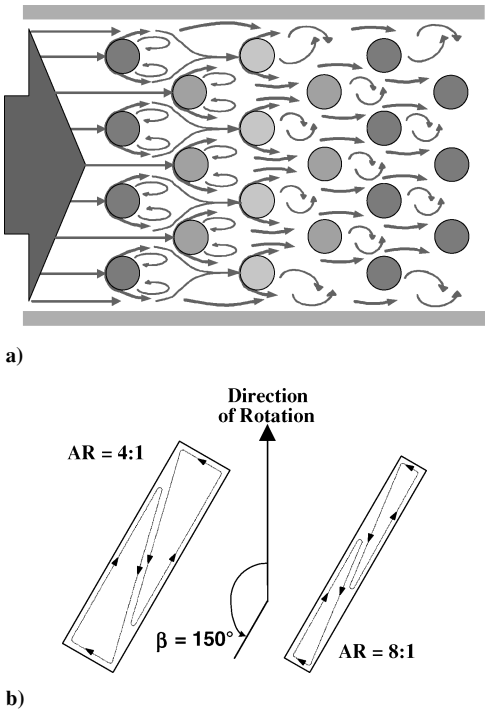

Fig. 4 Flow conceptualization: a) secondary flow induced by pin fins and b) vortices induced by rotation in rectangular channels.

thus, for the present study, the inner and outer surfaces were left unheated.

Secondary Flow Behavior

As shown in previous studies, the heat transfer trends within a pin fin channel are unlike those of a smooth channel. In a smooth channel, the maximum heat transfer occurs at the beginning of heated portion of the test section, and as the boundary layer develops, the Nusselt number gradually decreases until it becomes fully developed, at which point the Nusselt number will remain constant. However, in the case of the pin fins, the maximum Nusselt number is typically reached near the third row of pins, as shown by Metzger et al.[5]

The heat transfer associated with the first row of pin fins is primarily due to the thermal boundary layer that began just upstream. Figure 4a shows a flow conceptulization that as the flow continues around the pin fins in the first row, separation occurs, and wakes are formed in the flow just downstream of the first row. These wakes cause the heat transfer of the second row to increase. As the flow continues around the second row, separation occurs, and more wakes are formed downstream of the second row of pin fins. The wakes created by the first and second rows of pins affect the third row, and so the third row also sees increased heat transfer. Downstream of the third row, the fluid is sufficiently mixed, that so as the flow continues downstream, the Nusselt number slightly decreases until reaching its fully developed value.

The Coriolis and buoyancy forces, induced by the rotation, effect the flow through a rotating channel. Two counter-rotating vortices are created in a smooth rotating channel. The vortices are created as a result of the coolant being forced from the leading-inner corner to the trailing-outer corner. The rotation-induced vortices can be seen in Fig. 4b. Figure 4b also emphasizes change in flow behavior with the change in channel aspect ratio. As one might expect, the size of the counter-rotating vortices decreases as the aspect ratio increases, but the general behavior of the secondary flow is similar. The trailing surfaces experience enhanced heat transfer as the coolant is forced to the trailing side of the channel, and the trailing-outer surface typically experiences the greatest enhancement. However, because of the rectangular channel and orientation angle, the leading surface should also experience heat transfer enhancement.

It is uncertain how the secondary flow in the pin fin channel will be effected by rotation. Because the pins span the entire cross section of the channel (extend from the leading surface to the trailing surface), there will be less structure to the counter-rotating vortices that are typically formed in the rotating channel. Because the cross section of the channel is partially obstructed, the coolant simply cannot be forced from the leading-inner corner of the channel to the trailing-outer corner. As the coolant begins to move from the leading surface, its path is obstructed by the pins; therefore, the coolant is forced to take a path around the pins. This obstructed path of the coolant will cause the trailing surface of the channel to experience less heat transfer enhancement than a smooth channel due to rotation. Therefore, in the rotating pin fin channels, the majority of heat transfer enhancement is expected to be the result of the secondary flow induced by the pin fins, rather than the rotational induced secondary flow.

Although the use of nonconducting pin fins is not practical to the design of actual turbine blades, they offer an interesting research perspective. The use of nonconducting (Plexiglas pins) allows for separation of the leading and trailing surfaces. Therefore, the heat transferred from the endwalls is the result of the turbulence generated by the pins. Under rotating conditions, the amount of heat transferred from the leading surface to the trailing surface is limited due to the very low conductivity of the pin fins. From the basic fin heat transfer analysis, it was estimated that only 5% of net heat input is dissipated through the nonconducting pin fins. In contrast, approximately 45% of the net heat input is transferred to the conducting pin fins.

Stationary Channel Results

Figures 5–7 contain the stationary Nusselt number ratio results for the smooth, nonconducting, and conducting pin fin channels. Each of Figs. 5–7 represents four experiments: 1) $Re = 5 \times 10^3$, 2) $Re = 1 \times 10^4$, 3) $Re = 1.5 \times 10^4$, and 4) $Re = 2 \times 10^4$. Note that the Nusselt number ratio in Figs. 5–7. is based on the hydraulic diameter.

Figures 5 and 6 show the stationary pin fin and smooth channel results for the 4:1 aspect ratio channel. As seen in Figs. 5 and 6,

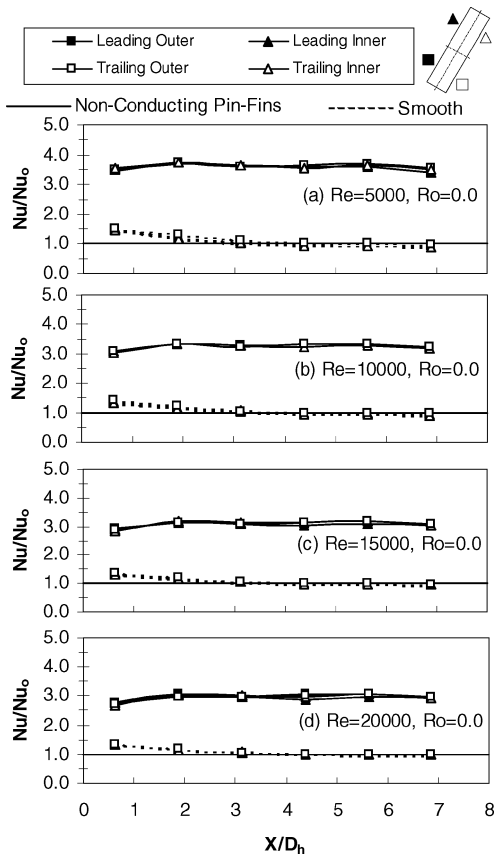

Fig. 5 Nusselt number ratio for stationary smooth and nonconducting pin-fin cases, *AR* = 4:1.

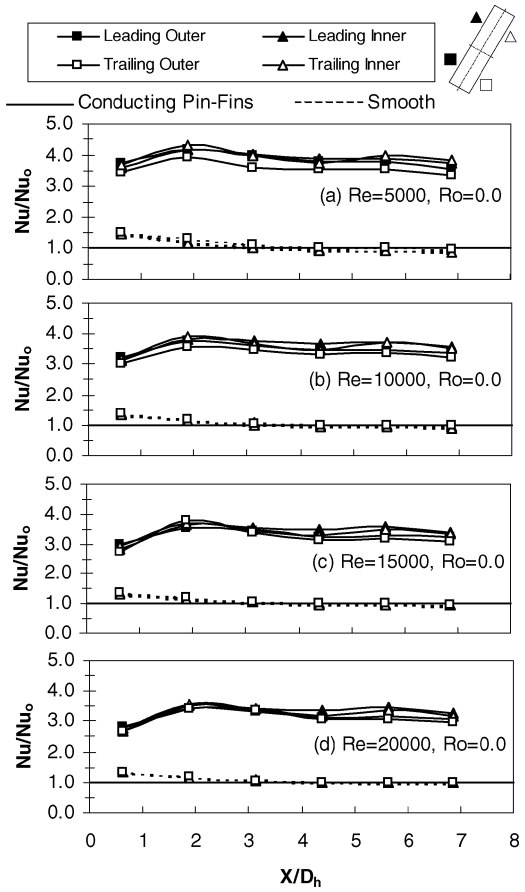

Fig. 6 Nusselt number ratio for stationary smooth and conducting pin fin cases, *AR* = 4:1.

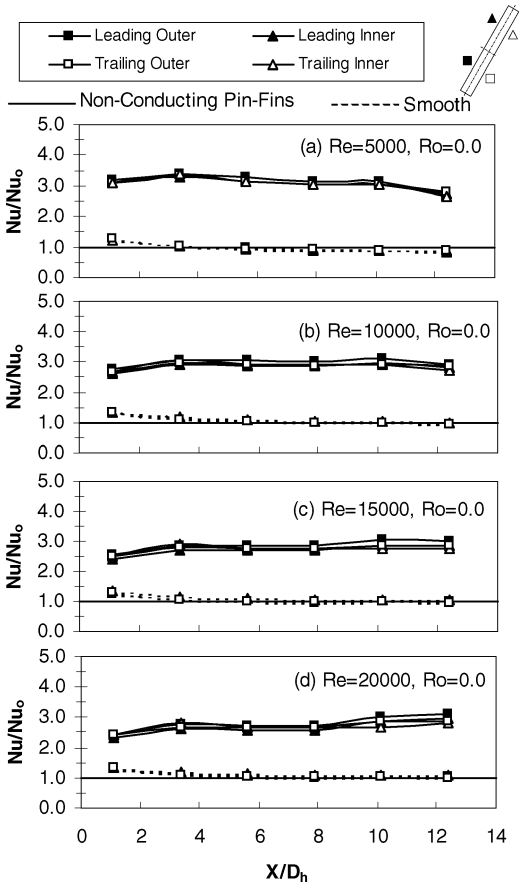

Fig. 7 Nusselt number ratio for stationary smooth and nonconducting pin fin cases, *AR* = 8:1.

the heat transfer trends through smooth and pin fin channels are quite different. Heat transfer in a smooth channel has a maximum value at the beginning of the channel due to the thermal development of the flow in this entrance portion of the heated test section, and it gradually decreases until it reaches the fully developed value of unity. However, in pin fin channels, the heat transfer increases to maximum value before it begins to decrease and then stabilize due to the separation and wake formation around the pins. Figure 5 shows that the nonconducting pin fins enhance heat transfer up to 3.2 times that of a smooth duct. As shown in Fig. 6, the conducting pin fins enhance heat transfer up to 3.8 times that of a smooth duct. In the case of the conducting pin fins, heat is transferred, by forced convection, from both the endwalls of the channel and the pin fins. The total surface area of the 4:1 conducting pin fin channel is increased by 52% when compared to the smooth channel. In contrast, within the nonconducting pin fin channel, the heat is primarily transferred from the endwalls; however, due to the relatively short length of the pin, it is reasonable to assume that some heat is lost through the Plexiglas pins themselves. As stated earlier, by the use of these surface area definitions, a more accurate representation of the regional heat transfer enhancement is presented.

Figure 7 shows the Nusselt number ratios for the 8:1 smooth channel, as well as the 8:1 channel with nonconducting pin fins. The general trends demonstrated in the streamwise direction are the same as those in the 4:1 channels. The heat transfer in the 8:1 channel with nonconducting pin fins is enhanced up to three times that of the smooth channel. These results are comparable to those of the 4:1 channels. Because of the similarity in results of the three pin-fin channels, an investigation of the 8:1 channel with conducting pin fins was not pursued.

Figure 8 compares the present pin fin data to several previous studies. The array averaged Nusselt numbers are plotted as a function of Reynolds number based on the pin diameter (Re_{D_p}). Both correlations presented by Metzger et al.[5,7] are relevant to conductive

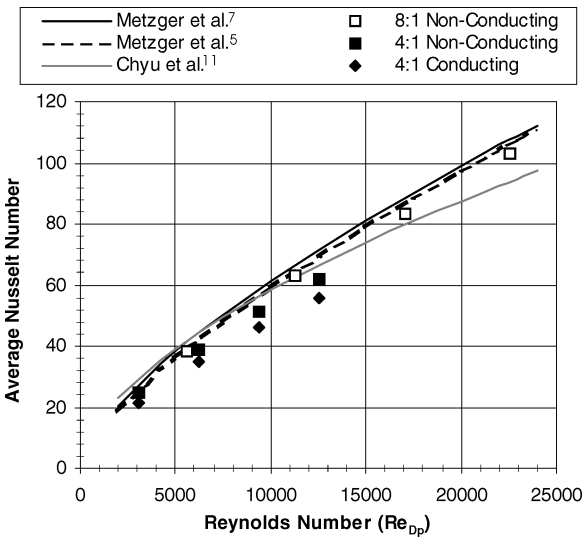

Fig. 8 Array averaged Nusselt number for stationary pin cases.

pin fin arrays. The surface area used to calculate the heat transfer coefficient is the exposed copper area; this area definition was also used by Metzger et al. in both cited studies. To compare the present study to the study of Chyu et al.,[11] which isolated the endwall heat transfer, it is necessary to consider only the exposed copper of the endwalls. Therefore, the surface area used to calculate the Nusselt number, in the nonconducting arrays, is only the exposed copper area ($A_{\mathrm{cu,pl}} - A_{c,b}$). As shown in Fig. 8, the results from the 8:1 nonconducting pin-fin channel are consistent with the result from the previous studies. The results from the 4:1 channel are comparable to the previous studies; however, they do not correlate as well as

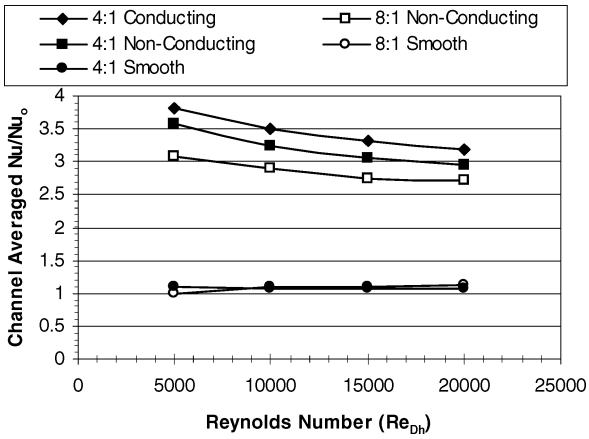

Fig. 9 Channel averaged Nusselt number ratio for all stationary cases.

the 8:1 results. The 4:1 nonconducting values are within 12% of the correlations, and the 4:1 conducting values are within 20% of the correlations. This difference can be explained because the geometry of the present study and the previous studies are not identical. Experimental uncertainty will also introduce differences in the data. Figure 8 also shows that the nonconducting channels generate the greatest enhancement. This varies from the Figs. 5–7 because the surface area definition was altered. By inclusion of only the exposed copper as the surface area, the total surface decreased, and, thus, the heat transfer coefficient increased.

The channel averaged Nusselt number ratio is shown in Fig. 9. Unlike Fig. 8, Fig. 9 presents the heat transfer enhancement based on the hydraulic diameter of the channel and the surface area described in conjunction with Figs. 5–7. Note that the Nusselt number ratio decreases as the Reynolds number increases. In addition, the 4:1 channel with conducting pin fins displays the greatest heat transfer enhancement, followed by the 4:1 and the 8:1 nonconducting pin fins, respectively. The channel averaged results for the smooth channel are elevated above the anticipated value of unity due to the entrance effect within the channel. As shown in Figs. 5–7, the heat transfer ratio is at a maximum at the entrance of the smooth channel, and it gradually decreases to the fully developed value of unity.

Rotating Channel Results

Figures 10–12 present the Nusselt number ratios for the pin fin and smooth channels under rotation. Figure 10 contains the results for the nonconducting pin fin and smooth channels with the 4:1 aspect ratio. The general trends of the data for the smooth channel are the same as for the stationary cases. However, at the higher rotation numbers (lower Reynolds numbers), there exists spanwise variation. At the Reynolds number of 5×10^3 ($Ro = 0.302$), all surfaces within the smooth channel experience heat transfer enhancement. Moreover, as one may anticipate, the surface that undergoes the least enhancement is the leading-inner surface. As was explained earlier, this is due to the rotation-induced vortices that shift the coolant away from the leading-inner corner to the trailing-outer corner of the channel. As the rotation number decreases, rotation has less of an effect on the coolant flow through the channel. At the Reynolds number of 2×10^4 ($Ro = 0.075$), the spanwise variation is very small, and the flow in the smooth rotating channel exhibits the same trend as the flow in the smooth stationary channel, namely, a gradual decrease until the fully developed value of unity is achieved.

The results for the 4:1 nonconducting pin fin channel, also shown in Fig. 10, are similar to those of the smooth channel. Spanwise variation is only present at the highest rotation number. However, there exists less spanwise separation in the pin fin channel as compared to the smooth channel. A maximum variation of 11% exists within the pin fin channel, and a maximum variation of 34% can be seen in the smooth channel. This is due to the pin fins themselves. Because the pins extend completely across the channel (from the

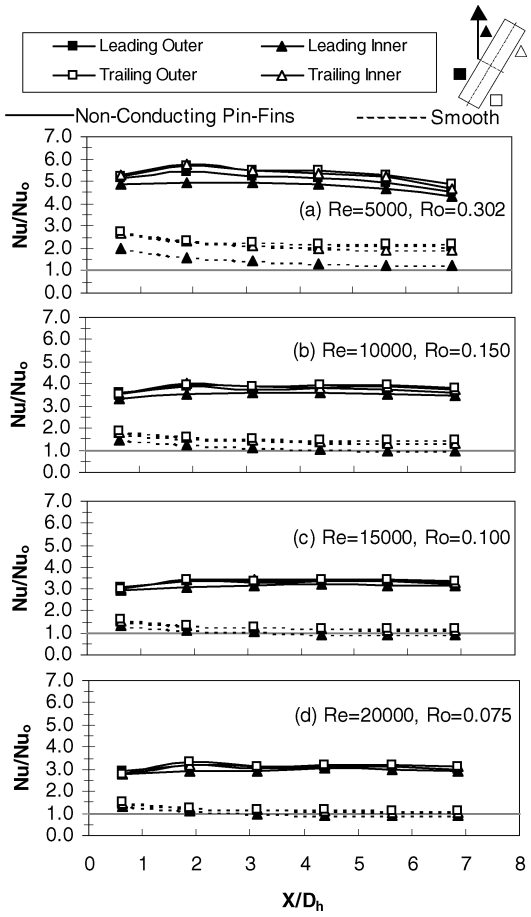

Fig. 10 Nusselt number ratio for rotating smooth and nonconducting pin fin cases, *AR* = 4:1.

leading surface to the trailing surface), there is not complete formation of the rotation induced vortices, as there is in the smooth channel. In other words, the presence of the pin fins limits the movement and circulation of the fluid from the leading-inner corner to the trailing-outer corner of the channel. As with the smooth channel, all surfaces undergo heat transfer enhancement as compared to the stationary channels. The greatest enhancement is seen in the trailing surface of the channel, and, as the rotation number decreases, the enhancement in the pin fin channels also decreases.

The results for the rotating 4:1 channel with conducting pin fins can be seen in Fig. 11. Again, at the lowest Reynolds number (highest rotation number), spanwise variation is present. However, the greatest separation occurs with the trailing-inner surface; this surface experiences the greatest enhancement. Although there is a lack of clearly defined vortices induced by rotation, the Coriolis forces continue to force the coolant away from the leading surface toward the trailing surface. In this channel, with the conducting pin fins (Fig. 11), the effect of rotation is more clearly seen by the enhancement of the trailing surface, or more specifically by the trailing-inner surface, rather than the declination of the leading surface. As is the case with both the smooth and nonconducting pin fin 4:1 channels (Fig. 10), all cases in the conducting pin fin channel (Fig. 11) undergo heat transfer enhancement as compared to the stationary cases, and, as the rotation number decreases, the heat transfer enhancement (as compared to the stationary channel) also decreases.

Figure 12 shows the results for the smooth and nonconducting pin-fin channels with an aspect ratio of 8:1. This very narrow channel yields much lower rotation numbers than the 4:1 channels. Therefore, the effect of rotation on the 8:1 channel is less evident than on the 4:1 channel. For the 8:1 smooth channel, note that the Nusselt number ratio for the leading-inner surface reaches a fully developed value below unity for all four cases. The rotation induced vortices

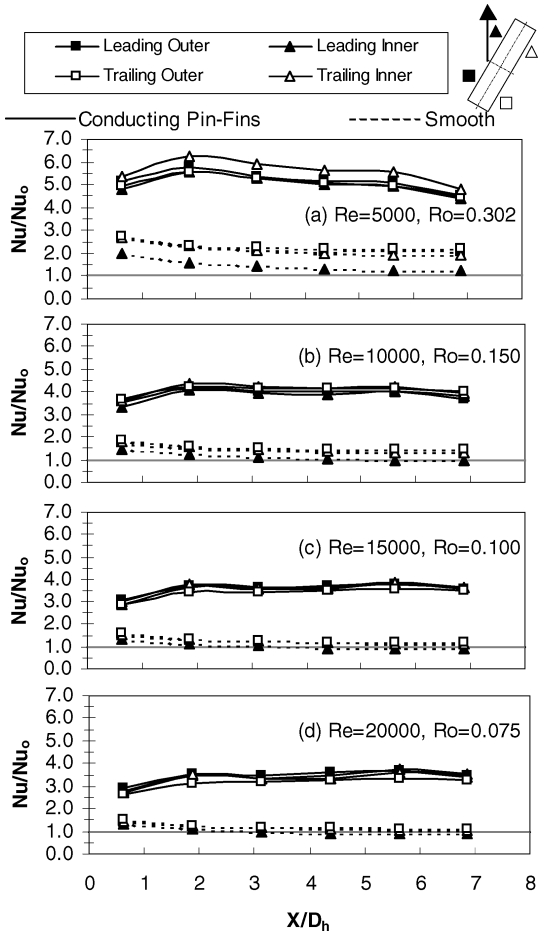

Fig. 11 Nusselt number ratio for rotating smooth and conducting pin fin cases, *AR* = 4:1.

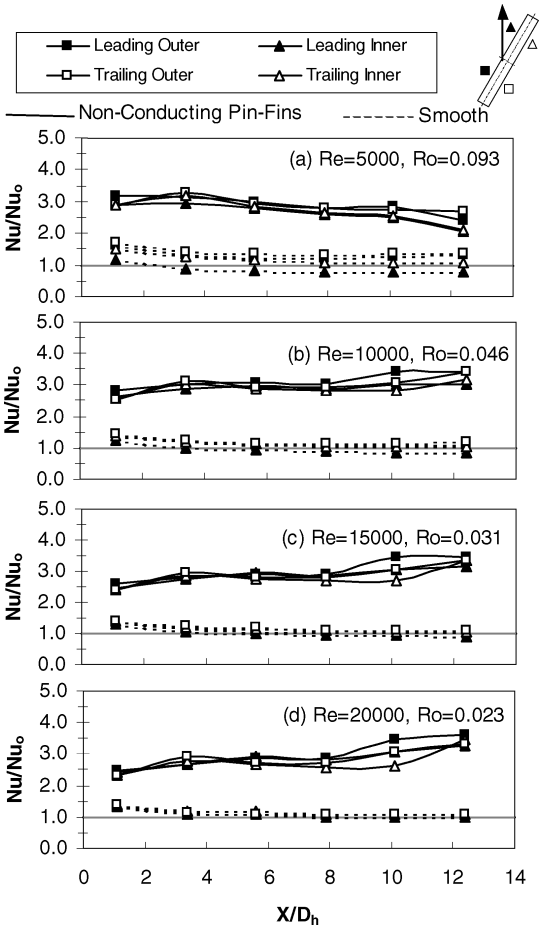

Fig. 12 Nusselt number ratio for rotating smooth and nonconducting pin fin cases, *AR* = 8:1.

are forcing the coolant from the leading-inner corner to the trailing-outer corner, and so coolant is being forced away from the leading-inner surface. For the case with the rotation number of 0.093, where the spanwise variation is most evident, all of the remaining surfaces (leading-outer, trailing-outer, and trailing-inner) experience heat transfer enhancement compared to the stationary smooth channel. The spanwise variation that is evident at the higher rotation numbers diminishes as the rotation number decreases (Reynolds number increases).

For the nonconducting pin fin channel with aspect ratio of 8:1, a small amount of spanwise variation exists. In all four cases, the trailing-outer and leading-outer surfaces undergo greater heat transfer enhancement than the leading-inner and trailing-inner surfaces. The spanwise variation is not as pronounced in the 8:1 pin fin channel as it is in the 4:1 pin fin channels. Because of the very narrow cross section of the 8:1 channel, the rotation numbers at the specified Reynolds numbers are much lower than the corresponding rotation numbers of the 4:1 channels. As with the 4:1 pin fin channels, the presence of pins obstructs the formation of the rotation induced vortices that are present in the smooth channel. The effect of rotation is more clearly seen by comparison of the Nusselt number ratios of the 8:1 rotating pin fin channel to those of the corresponding stationary channel.

Figures 13–15 show the streamwise averaged Nusselt number ratios for the smooth, nonconducting pin fin, and conducting pin fin channels, respectively. Figure 13 shows the streamwise averaged Nusselt number ratio for the smooth channel. The leading-inner surface of the 8:1 channel experiences a declination in heat transfer with the increasing effect of rotation; however, in the 4:1 channel, the leading-inner surface experiences heat transfer enhancement. This is the result of the vortices induced by rotation. The coolant is clearly forced away from the leading-inner surface toward the other

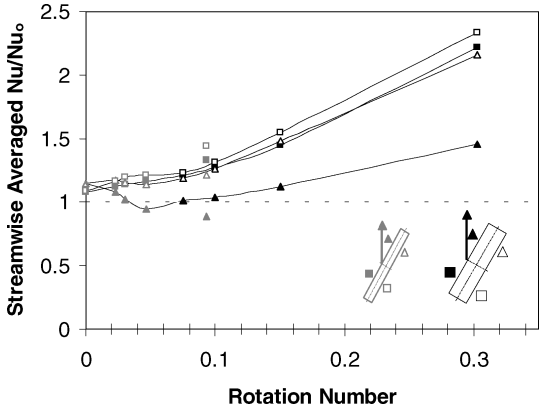

Fig. 13 Streamwise averaged Nusselt number ratio for the smooth rotating channel.

surfaces of the channel. Therefore, each of the remaining surfaces experience heat transfer enhancement with an increase in rotation number. The spanwise variation is also clearly seen in Fig. 13. As the rotation number continues to increase, the separation between the surfaces increases. The enhancement for the trailing surfaces and the leading-outer surface is much greater than the enhancement of the leading-inner surface.

The streamwise averaged Nusselt number ratios for the nonconducting pin-fin channels are shown in Fig. 14. In general, all surfaces experience heat transfer enhancement with an increase in rotation number. The only exception, as stated earlier, is in the 8:1 channel at the rotation number of 0.093. As is the case with the smooth channel, spanwise variation, in the present channel, increases as the

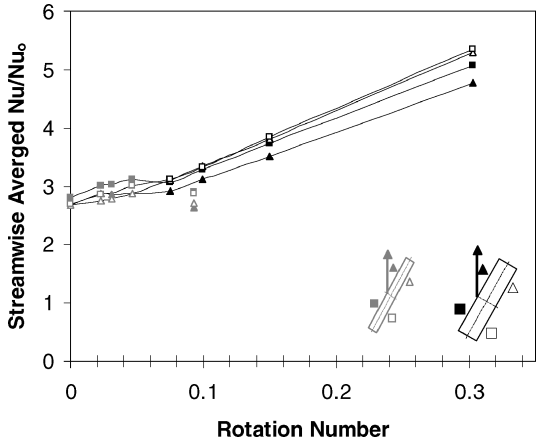

Fig. 14 Streamwise averaged Nusselt number ratio for the rotating channel with nonconducting pin fins.

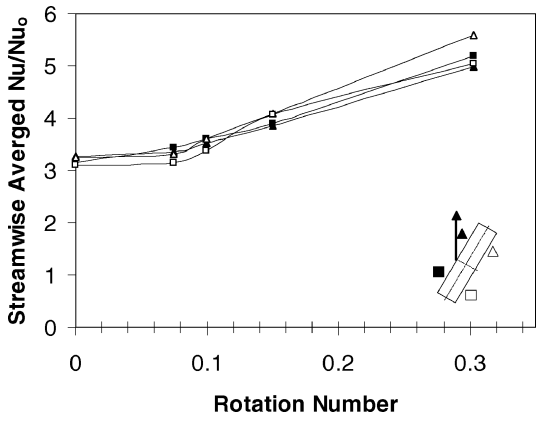

Fig. 15 Streamwise averaged Nusselt number ratio for the rotating channel with conducting pin fins.

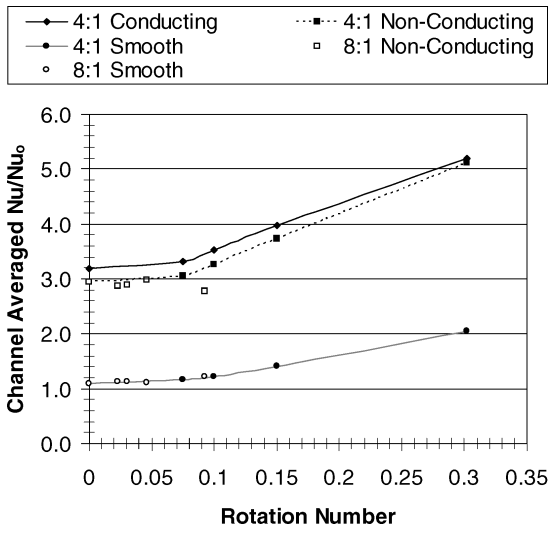

Fig. 16 Channel averaged Nusselt number ratio for smooth and pin fin cases.

rotation number increases. The greatest heat transfer enhancement occurs in the trailing-outer and trailing-inner surfaces, followed by the leading-outer surface and leading-inner surface, respectively.

Figure 15 shows the streamwise averaged results for the 4:1 channel with conducting pin fins. The Nusselt number ratios and trends are similar to those of the nonconducting pin fin channel. All surfaces undergo heat transfer enhancement with the increasing rotation number. Also, the greatest spanwise variation exists at the highest rotation number; at this location, the trailing-inner surface experiences greater heat transfer enhancement than the other surfaces.

Figure 16 presents the channel averaged Nusselt number ratios; this is the average of the leading and trailing surfaces within the channel. It is clear that a greater amount of heat is transferred from the wall of the channel with conducting pin fins than the channel with nonconducting pin fins. However, the enhancement due to rotation is the same for both channels.

Conclusions

1) For the pin fin channels, the greatest heat transfer enhancement is due to the turbulent heat transfer created by the pin fins. The Nusselt number ratio in the stationary pin-fin channels is up to 3.8 times greater than the ratios in the smooth stationary channels.

2) Overall, all surfaces in the smooth rotating channels experience heat transfer enhancement compared to the stationary smooth channels. In the smooth channel, the trailing-outer surface experiences the greatest heat transfer enhancement due to rotation. This is followed by the trailing-inner, leading-outer, and leading-inner surfaces, respectively.

3) Because of the channel geometry, aspect ratios, and orientation angle, the heat transfer from all surfaces of the pin fin channels is enhanced with rotation. The enhancement can be as much as two times the enhancement of the stationary pin fin channels. The rotation numbers for the 4:1 channels are greater than the rotation numbers for the 8:1 channels; therefore, the effect of rotation is more evident.

4) The Nusselt number ratios for the conducting pin fin channel are greater than those of the nonconducting pin fin channel. However, as the rotation number increases, the Nusselt number ratios, for both of the pin fin channels, increases at the same rate.

5) Spanwise variation is most predominant in the smooth channel. Variation exists in the pin fin channels, but the variation is less than that of the smooth channel due to the obstructions created by the pins.

Acknowledgments

This publication was prepared wit the support of the U.S. Department of Energy (DOE), Office of Fossil Energy, National Energy Technology Laboratory. However, any opinions, findings, conclusions, or recommendations expressed herein are those of the authors and do not necessarily reflect the views of the DOE.

References

[1]Wagner, J. H., Johnson, B. V., and Hajek, T. J., "Heat Transfer in Rotating Passages with Smooth Walls and Radial Outward Flow," *Journal of Turbomachinery*, Vol. 113, No. 1, 1991, pp. 42–51.

[2]Dutta, S., Han, J. C., Zhang, Y., and Lee, C. P., "Local Heat Transfer in a Rotating Two-Pass Triangular Duct with Smooth Walls," *Journal of Turbomachinery*, Vol. 118, No. 3, 1996, pp. 435–443.

[3]Willett, F. T., and Bergles, A. E., "Heat Transfer in Rotating Narrow Rectangular Ducts with Heated Sides Oriented at 60° to the R–Z Plane," *ASME Journal of Turbomachinery*, Vol. 123, No. 2, 2001, pp. 288–295.

[4]Griffith, T. S., Al-Hadhrami, L., and Han, J. C., "Heat Transfer in Rotating Rectangular Cooling Channels ($AR = 4$) with Angled Ribs," *Journal of Heat Transfer*, Vol. 124, No. 4, 2002, pp. 617–625.

[5]Metzger, D. E., Berry, R. A., and Bronson, J. P., "Developing Heat Transfer in Rectangular Ducts with Staggered Arrays of Short Pin Fins," *Journal of Heat Transfer*, Vol. 104, No. 4, 1982, pp. 700–706.

[6]Metzger, D. E., and Haley, S. W., "Heat Transfer Experiments and Flow Visualization for Arrays of Short Pin Fins," American Society of Mechanical Engineers, ASME Paper 82-GT-138, 1982.

[7]Metzger, D. E., Shepard, W. B., and Haley, S. W., "Row Resolved Heat Transfer Variations in Pin-Fin Arrays Including Effects of Non-Uniform Arrays and Flow Convergence," American Society of Mechanical Engineers, ASME Paper 86-GT-132, 1986.

[8]VanFossen, G. J., "Heat-Transfer Coefficients for Staggered Arrays of Short Pin Fins," *Journal of Engineering for Power*, Vol. 104, No. 2, 1982, pp. 268–274.

[9]Brigham, B. A., and VanFossen, G. J., "Length to Diameter Ratio and Row Number Effects in Short Pin Fin Heat Transfer," *Journal of Engineering for Gas Turbines and Power*, Vol. 106, No. 1, 1984, pp. 241–245.

[10]Chyu, M. K., and Hsing, Y. C., "Convective Heat Transfer of Cubic Fin Arrays in a Narrow Channel," *Journal of Turbomachinery*, Vol. 120, No. 2, 1998, pp. 362–367.

[11]Chyu, M. K., Hsing, Y. C., and Shih, T. I.-P., "Heat Transfer Contributions of Pins an Endwall in Pin-Fin Arrays: Effects of Thermal Boundary Condition Modeling," *ASME Journal of Turbomachinery*, Vol. 121, No. 2, 1999, pp. 257–263.

[12]Uzol, O., and Camci, C., "Elliptical Pin Fins as an Alternative to Circular Pin Fins for Gas Turbine Blade Cooling Applications, Part 1: Endwall Heat Transfer and Total Pressure Loss Characteristics," American Society of Mechanical Engineers, ASME Paper 2001-GT-0180, 2001.

[13]Willet, F. T., and Bergles, A. E., "Heat Transfer in Rotating Narrow Rectangular Pin-Fin Ducts," *Experimental Thermal and Fluid Science*, Vol. 25, No. 7, 2002, pp. 573–582.

[14]Han, J. C., Dutta, S., and Ekkad, S. V., *Gas Turbine Heat Transfer and Cooling Technology*, Taylor and Francis, New York, 2000.

[15]Kline, S. J., and McClintock, F. A., "Describing Uncertainties in Single-Sample Experiments," *Mechanical Engineering*, Vol. 75, Jan. 1953, pp. 3–8.